Fermi National Accelerator Laboratory

FERMILAB-Pub-90/81-A
May 1990

AXIONS AND SN 1987A: AXION TRAPPING

Adam Burrows,[a] *M. Ted Ressell,*[b,c] *and Michael S. Turner*[b,c,d]

[a]Department of Physics and Astronomy
University of Arizona
Tucson, AZ 85721

[b]Department of Astronomy and Astrophysics
The University of Chicago
Chicago, IL 60637-1433

[c]NASA/Fermilab Astrophysics Center
Fermi National Accelerator Center
P.O. Box 500
Batavia, IL 60510-0500

[d]Department of Physics
Enrico Fermi Institute
The University of Chicago
Chicago, IL 60637-1433

Abstract. If an axion of mass between about 10^{-3} eV and 1 eV exists, axion emission would have significantly affected the cooling of the nascent neutron star associated with SN 1987A. For an axion of mass less than about 10^{-2} eV axions produced deep inside the neutron star simply stream out; in a previous paper we have addressed this case. Remarkably, for an axion of mass greater than about 10^{-2} eV axions would, like neutrinos, have a mean-free path that is smaller than the size of a neutron star, and thus would become "trapped" and radiated from an "axion sphere." In this paper we treat the "trapping regime" by using numerical models of the initial cooling of a hot neutron star that incorporate a "leakage" approximation scheme for axion-energy transport. We compute the axion opacity due to inverse nucleon-nucleon, axion bremsstrahlung, and then use our numerical models to calculate the integrated axion luminosity, the temperature of the axion sphere, and the effect of axion emission on the neutrino bursts detected by the Kamiokande II (KII) and Irvine-Michigan-Brookhaven (IMB) water-Cherenkov detectors. The larger the axion mass, the stronger the trapping and the smaller the axion luminosity. We confirm and refine the earlier estimate of the axion mass above which trapping is so strong that axion emission does not significantly affect the neutrino burst: Based upon the neutrino-burst duration—the most sensitive "barometer" of axion cooling—we conclude that for an axion mass of greater than about 0.3 eV axion emission would not have had a significant effect on the neutrino bursts detected by KII and IMB. The present work, together with our previous work, strongly suggests that an axion with mass in the interval 10^{-3} eV to 0.3 eV is excluded by SN 1987A.

I. Introduction

Peccei-Quinn (PQ) symmetry may be the simplest and most compelling extension of the standard $SU(3)_C \otimes SU(2)_L \otimes U(1)_Y$ model. PQ symmetry cures the single blemish on QCD: the strong-CP problem, and predicts the existence—but not the mass—of a new pseudoscalar particle: the axion.[1] A priori the mass of the axion could be anywhere between about 10^{-12} eV and 1 MeV, corresponding to PQ symmetry breaking scales between about 10^{19} GeV and 100 GeV. (The axion mass and PQ symmetry breaking scale are related by $m_a/\mathrm{eV} \simeq 6 \times 10^6\,\mathrm{GeV}/(f_a/N)$; the axion coupling to ordinary matter is proportional to m_a—or equivalently, $(f_a/N)^{-1}$.) A host of astrophysical and cosmological arguments—and a few laboratory searches—have left open but two "windows" for the axion mass: 10^{-6} eV to 10^{-3} eV and about 1 eV to 5 eV (hadronic axion only); see Refs. 2 for an up-to-date review of the "axion window." One of the most powerful and important constraints to the axion mass is based upon the early cooling of the neutron star associated with SN 1987A. Axion emission can accelerate the cooling of the nascent neutron star and thereby shorten the neutrino burst. In particular, it has been argued that the neutrino bursts detected by the Kamiokande II (KII) and Irvine-Michigan-Brookhaven (IMB) water-Cherenkov detectors would have been significantly shorter than the bursts actually observed if an axion in the mass interval of 10^{-3} eV to 2 eV existed.[3] (Many authors have studied the possible effect of axions on the cooling of SN 1987A; Ref. 4 contains a semi-complete bibliography.)

At the temperatures and densities relevant to the hot, newly born neutron star, the dominant process for axion emission (and absorption) is nucleon-nucleon, axion bremsstrahlung (and inverse axion bremsstrahlung): $N + N \leftrightarrow N + N + a$. Axion emission from the nascent neutron star can be divided into two qualitatively different regimes: "freely streaming," for $m_a \lesssim 0.01$ eV; and "trapping," for $m_a \gtrsim 0.01$ eV. In the freely streaming regime the axion-mean-free path for absorption is large compared to the size of the neutron star, and axions, once emitted, simply "freely stream" into the vacuum of space. In the trapping regime, axions interact sufficiently strongly that their mean-free path for absorption is small compared to the size of the neutron star; in this case, like neutrinos, they are said to be "trapped" and are effectively emitted from an axion sphere. (The axion sphere is the surface beyond which the probability for an axion to be absorbed is 2/3.)

Neglecting the "back reaction" of axion emission on the cooling of the neutron star, axion emission in the freely streaming regime is simply proportional to the axion-nucleon coupling squared which is proportional to the axion mass squared. In the trapping regime things are more complicated; in the simplest treatment, the axion luminosity is proportional to the fourth power of the temperature of the axion sphere. Based upon a simple analytic model[3] (which this work shows to be quite good) it has been argued that the temperature of the axion sphere varies as $m_a^{-4/11}$, so that the axion luminosity in the trapping regime should vary as $m_a^{-16/11}$. Roughly then, one expects that as a function of

axion mass, the axion luminosity should increase as m_a^2 for $m_a \ll 10^{-2}$ eV, and should decrease as $m_a^{-16/11}$ for $m_a \gg 10^{-2}$ eV (see Fig. 1). From this simple picture, one sees that here should be two "critical" masses for axion emission from SN 1987A: one below which axion emission is acceptable because the axion interacts so weakly; and one above which axion emission is again acceptable because the axion interacts so "strongly."

The freely streaming regime is relatively simple to treat: A heat sink of magnitude equal to the local axion-emission rate is incorporated into numerical models of nascent neutron star cooling. In previous work we did just that.[5] Based upon the duration of the neutrino bursts that would have been observed in the KII and IMB detectors we concluded that the "lower mass boundary" is about 10^{-3} eV . (Several other studies are in agreement with our conclusion.[4]) The trapping regime is more difficult to address because in principle one has to treat axion-energy transport in much the same way as one does neutrino-energy transport (or radiative transport in an ordinary star). Based upon a simple analytic model the "upper mass boundary" was estimated to be about 2 eV.[3] The existence of the previously mentioned axion window around a few eV depends crucially upon the upper mass boundary: Were it 5 eV rather than 2 eV the window would be closed. Moreover, two experiments have been proposed to search for axions in this mass range. The first involves searching for the photon-line radiation produced by the decays of relic (cosmological) axions;[6] and the second involves detecting axions emitted by the sun by axion-photon conversion induced by a strong magnetic field.[7] For this reason, and the general importance of the SN 1987A bound to the axion mass, we are addressing axion transport and emission in the trapping regime.

To preview our results, the window doesn't "close up," rather it "opens up:" Based upon the present work we conclude that the upper boundary mass is about 0.3 eV, rather than the original estimate of about 2 eV. The present work together with our previous work[5] strongly suggests that the durations of the neutrino bursts detected by KII and IMB exclude an axion with mass in the interval 10^{-3} eV to 0.3 eV. We are quick to remind the reader that both mass boundaries depend upon the precise form of the axion-nucleon coupling, as well as the neutron star models and the exact burst-duration exclusion criterion. The mass boundaries are therefore "fuzzy" by about a factor of three.

The outline of the rest of the paper is as follows. In the next Section we will calculate the crucial physics input to the problem: the axion opacity (under ordinary circumstances, this would be an oxymoron). In Section III we will derive the equations that govern axion transport and the "leakage" approximation scheme that we will employ. Section IV is devoted to a discussion of the results of our numerical simulations of axion-cooled neutron stars, and in Section V we summarize and add some concluding remarks.

II. Axion Opacity

As we have discussed above, for an axion mass of greater than about 10^{-2} eV, it is expected that the axion-mean-free path for absorption (at densities and temperatures

typical of a newly born neutron star) is less than the radius of a neutron star.[3] In this mass regime axions do not simply stream out and one has to calculate the axion luminosity in much the same way one does the photon luminosity in an ordinary star or the neutrino luminosity in a newly born, hot neutron star. To do so one needs to calculate the axion opacity as a function of density, ρ, temperature, T, and the axion energy, E_a. The axion opacity, κ_E, at energy E_a is related to the axion-mean-free path by

$$(\kappa_E \rho)^{-1} \equiv \lambda_a(E_a, \rho, T). \tag{1}$$

In the present circumstance, unlike photon transport in an ordinary star or neutrino transport in a hot neutron star, only absorption is important. This is because each axion line in a Feynman diagram introduces a dimensionless coupling factor of order $m_N/(f_a/N) \sim 10^{-7}(m_a/\mathrm{eV})$, and so processes involving more than one axion are suppressed relative to those involving a single axion by a factor of at least $10^{-14}(m_a/\mathrm{eV})^2$. By far the dominant axion-absorption process is inverse nucleon-nucleon, axion bremsstrahlung ($a + N + N \rightarrow N + N$; N is a neutron or proton).

There are two equivalent methods for computing λ_a. The first, more familiar to a physicist, relies upon the Boltzmann equation:

$$\lambda_a^{-1} \equiv f_a^{-1}\frac{\partial f_a}{\partial t} = \frac{1}{2E_a}\int d\Pi_1 d\Pi_2 d\Pi_3 d\Pi_4 (2\pi)^4 \delta^4(p_a + p_1 + p_2 - p_3 - p_4)$$

$$\times S|\mathcal{M}|^2 f_1 f_2 (1 - f_3)(1 - f_4), \tag{2}$$

where p_1, p_2, p_3, p_4 and p_a are the nucleon and axion four momenta, the subscripts 1, 2 (3, 4) refer to the incoming (outgoing) nucleons, $d\Pi_i = d^3p_i/(2\pi)^3 2E_i$ is the Lorentz-invariant phase-space-volume element, f_i are the nucleon-phase-space distribution functions, S is the symmetry factor (a factor of 1/2 for identical nucleons in the initial *or* final states), and $|\mathcal{M}|^2$ is the matrix-element squared (summed over initial and final spins). Throughout this Section we shall set $\hbar = k_B = c = 1$. For reference, we remind the reader that the axion-nucleon interaction follows from the Lagrangian density

$$\mathcal{L}_{\mathrm{int}} = \cdots + (g_{an}/2m_N)(\bar{n}\gamma_\mu\gamma_5 n)\partial^\mu a + (g_{ap}/2m_N)(\bar{p}\gamma_\mu\gamma_5 p)\partial^\mu a,$$

where the axion-nucleon couplings $g_{an} = c_n m_N/(f_a/N)$ and $g_{ap} = c_p m_N/(f_a/N)$, and c_p and c_n are numerical constants of order unity. For more about the axion and its couplings to ordinary matter see Refs. 8. For the derivation of the matrix element squared and the details of carrying out the phase-space integrations see Ref. 9.

The second method for computing λ_a, more familiar to an astrophysicist, relies upon Kirchhoff's law (also known as detailed balance or time-reversal invariance) for calculating the opacity,

$$\kappa_E = \frac{j_E}{d\rho_a(T)/dE}, \tag{3}$$

where λ_a is related to κ_E by Eq. (1), j_E is the axion emission rate (at energy E) per gram of material per second per axion energy interval, and

$$\frac{d\rho_a(T)}{dE_a} = \frac{1}{2\pi^2}\frac{E_a^3}{e^{E_a/T}-1}, \tag{4}$$

is the differential axion energy density for a thermal distribution of axions. (Expression (3) is probabaly even more familiar when written for photons: $j_\nu = 4\pi\kappa_{\nu a}B_\nu(T)$, where $B_\nu(T) \equiv 2h\nu^3/(e^{h\nu/kT}-1)c^2$ is the Planck function, $d\rho_\gamma/d\nu = 4\pi B_\nu/c$, and $\nu = E/h = E/2\pi$ is the frequency; also note that because axions are spinless particles, the Planck functions for photons and axions differ by a factor of 2.) The total *axion-volume-emission rate*, $\dot{\varepsilon}_a$ (used in previous work on axions and SN 1987A), is related to j_E by

$$\dot{\varepsilon}_a = \rho\int_0^\infty j_E dE_a, \tag{5a}$$

$$\dot{\varepsilon}_a = \int d\Pi_1 d\Pi_2 d\Pi_3 d\Pi_4 d\Pi_a (2\pi)^4\delta^4(p_1+p_2-p_3-p_4-p_a)E_a$$
$$\times S|\mathcal{M}|^2 f_1 f_2(1-f_3)(1-f_4)(1+f_a). \tag{5b}$$

To make the calculation of λ_a tractable we will make some approximations. First, we will assume that $|\mathcal{M}|^2$ is approximately constant; as discussed in Refs. 10 this is a reasonable approximation at the temperatures and densities of interest (we will have more to say about this below). Assuming that $g_a = g_{an} = g_{ap}$, $S|\mathcal{M}|^2$ is given by[9]

$$S|\mathcal{M}|^2 = \frac{64}{3}\frac{g_a^2\alpha_\pi^2}{m_N^2}(3-\beta) \tag{6a}$$

for $n+n+a \to n+n$ and $p+p+a \to p+p$, and

$$S|\mathcal{M}|^2 = \frac{256}{3}\frac{g_a^2\alpha_\pi^2}{m_N^2}(7-2\beta) \tag{6b}$$

for $n+p+a \to n+p$, where $\alpha_\pi \equiv (fm_N/m_\pi)^2 \simeq 56$ is the nucleon-pion coupling factor and β is a parameter that depends upon the degree of nucleon degeneracy. For completely degenerate nucleon matter $\beta \to 0$, and for non-degenerate matter $\beta \to 1.0845$; see the Appendix of Ref. 9 for further details. Next, we assume that the nucleons can be treated as being non-degenerate. Deep in the core this is a marginal approximation;[9] however further out, near the axion sphere ($T \sim 10\,\mathrm{MeV}$, $\rho \sim 10^{12}\mathrm{g\ cm^{-3}}$) where all the action is, this is a good approximation. (Ishizuka and Yoshimura[10] have recently computed λ_a in the degenerate limit.) We also assume that the nucleons are non-relativistic, which is a very good approximation throughout the star. (In Ref. 11 the fully-relativistic matrix element and phase-space integrations are compared to the non-relativistic matrix element and phase-space integrations.) Finally, in the most important region, that near the axion

sphere, the densities are such that many-body effects, e.g., reduction in the effective nucleon mass and variation of the pion-nucleon and axion-nucleon couplings, should not be significant (see Ref. 11). In sum, the ambient conditions near the axion sphere are such that the various approximations we make are well justified.

With these approximations it follows that:

$$f_i = \exp(y_i - u_i), \quad u_i = p_i^2/2m_N T, \quad y_i = (\mu_i - m_N)/T,$$

$$n_i = \frac{1}{\pi\sqrt{2\pi}}(m_N T)^{3/2} e^{y_i},$$

where n_i is the number density of nucleon species i (= n or p) and μ_i is the chemical potential of species i.

It is now straightforward to evaluate analytically expression (2) for λ_a^{-1}:

$$\lambda_a^{-1} = \frac{S|\mathcal{M}|^2}{2^5\pi^{3/2}} \frac{n_1 n_2}{m^{5/2}T^{1/2}} e^{E_a/T} \left(\frac{T}{E_a}\right) \int_{E_a/2T}^{\infty} du_- u_-^{1/2} (u_- - E_a/2T)^{1/2} e^{-2u_-}. \qquad (7)$$

(The integrals in expression (2) for λ_a^{-1} are evaluated in an analogous manner, and using the same notation, as those for $\dot{\varepsilon}_a$ are in Ref. 9.) The final integral factor which is a function of E_a/T can be expressed in terms of the modified Bessel function $K_1(x)$:[12]

$$e^{E_a/T} \left(\frac{T}{E_a}\right) \int_{E_a/2T}^{\infty} du_- u_-^{1/2} (u_- - E_a/2T)^{1/2} e^{-2u_-}$$

$$= \frac{1}{4} \left(\frac{T}{E_a}\right) \int_0^{\infty} e^{-x} (x + E_a/T)^{1/2} x^{1/2} dx,$$

$$= \frac{1}{8} \exp(E_a/2T) K_1(E_a/2T) \simeq \frac{1}{4} \frac{T}{E_a} \left(1 + \frac{E_a}{T}\right)^{1/2}, \qquad (8)$$

where the second expression is a useful empirical fit which has an accuracy of about 10%. Note that the axion-mean-free path is relatively insensitive to the axion energy and temperature, and varies roughly as

$$\lambda_a \propto T^{1/2} \frac{E_a/T}{(1 + E_a/T)^{1/2}}; \qquad (9)$$

this is in agreement with the original estimate made in Ref. 3. Note too that the inverse of the axion-mean-free path is proportional to the target-number density squared, rather the target-number density as one usually finds; this of course is because the absorption process has a three-body initial state with two target nucleons.

Because the axion is a boson, the presence of ambient axions will lead to stimulated emission of axions, *cf.* the factor of $(1 + f_a)$ in Eq. (5). Owing to this fact, the "net"

absorption (= true absorption less stimulated emission) is less than the true absorption calculated above, and a "reduced" absorption opacity is often defined. Assuming an ambient thermal distribution of axions, the reduced absorption opacity is

$$\kappa_E^* \equiv \kappa_E \left(1 - e^{-E_a/T}\right). \tag{10}$$

The quantity κ_E^* describes the net axion absorption as a flux of axions passes through matter. As one can readily see the reduced absorption opacity and the absorption opacity do not differ by a large factor since the typical axion energy $E_a \sim 3T$. It is also useful to define the Rosseland-mean opacity

$$\left\langle \frac{1}{\kappa} \right\rangle_R \equiv \int_0^\infty \frac{1}{\kappa_E^*} \frac{\partial^2 \rho_a(T)}{\partial E \partial T} dE \Big/ \int_0^\infty \frac{\partial^2 \rho_a(T)}{\partial E \partial T} dE, \tag{11}$$

which weights κ_E^* near the peak of the energy flux ($E_a = 4T$). Using the energy dependence of the axion-absorptive opacity computed above, cf. Eq. (7), we find numerically that

$$\left\langle \frac{1}{\kappa} \right\rangle_R = \left(\frac{1}{\kappa_E} \right) \Big|_{E_a = 4.73T}. \tag{12}$$

In order to compute the total axion opacity one must consider all three absorption processes ($n + n + a \rightarrow n + n$, $p + p + a \rightarrow p + p$, and $n + p + a \rightarrow n + p$); this is accomplished by adding the corresponding expressions for λ_a^{-1} from each process:

$$\lambda_a^{-1}(\text{total}) = \lambda_a^{-1}(nn) + \lambda_a^{-1}(pp) + \lambda_a^{-1}(np); \tag{13}$$

opacities, like the resistances of resistors in series, add. Finally, taking $g_{an} = g_{ap} = g_a = \frac{1}{2} m_N/(f_a/N) \simeq 7.6 \times 10^{-8} (m_a/\text{eV})$ and setting $\beta = 1.0$, we can evaluate $\lambda_a^{-1}(\text{total})$ numerically:

$$\lambda_a^{-1} = (4.8 \times 10^3 \text{cm})^{-1} \left(\frac{m_a}{\text{eV}}\right)^2 \left(\frac{T}{\text{MeV}}\right)^{-1/2} \left(\frac{\rho}{10^{14} \text{gcm}^{-3}}\right)^2 \times (1 + 8 X_n X_p) e^{E_a/2T} K_1(E_a/2T); \tag{14a}$$

$$\lambda_a^{-1} \simeq (2.4 \times 10^3 \text{cm})^{-1} \left(\frac{m_a}{\text{eV}}\right)^2 \left(\frac{T}{\text{MeV}}\right)^{-1/2} \left(\frac{\rho}{10^{14} \text{gcm}^{-3}}\right)^2 \times (1 + 8 X_n X_p) \left(\frac{T}{E_a}\right) \left(1 + \frac{E_a}{T}\right)^{1/2}; \tag{14b}$$

where X_n and X_p are the neutron and proton mass fractions, and in Eq. (14b) we have used our empirical expression for $\exp(E_a/2T) K_1(E_a/2T)$. For consistency with our previous work[5] we have taken $g_{an} = g_{ap} = \frac{1}{2} m_N/(f_a/N) \simeq 7.6 \times 10^{-8} (m_a/\text{eV})$; the axion couplings depend upon the type of axion—DFSZ or hadronic—and uncertainties in the

quark distribution functions. As we will remind the reader in our concluding remarks, our results depend upon the assumed values of the couplings—and can be rescaled for different assumed values of the axion-nucleon couplings. From Eqs. (14) we can compute the axion opacity at energy E_a

$$\kappa_E = 2.1 \times 10^{-18} \left(\frac{\mathrm{cm}^2}{\mathrm{g}}\right) \left(\frac{m_a}{\mathrm{eV}}\right)^2 \left(\frac{T}{\mathrm{MeV}}\right)^{-1/2} \left(\frac{\rho}{10^{14}\mathrm{gcm}^{-3}}\right) \times (1 + 8X_n X_p) e^{E_a/2T} K_1(E_a/2T); \tag{15a}$$

$$\kappa_E \simeq 4.2 \times 10^{-18} \left(\frac{\mathrm{cm}^2}{\mathrm{g}}\right) \left(\frac{m_a}{\mathrm{eV}}\right)^2 \left(\frac{T}{\mathrm{MeV}}\right)^{-1/2} \left(\frac{\rho}{10^{14}\mathrm{gcm}^{-3}}\right) \times (1 + 8X_n X_p) \left(\frac{T}{E_a}\right) \left(1 + \frac{E_a}{T}\right)^{1/2}. \tag{15b}$$

Finally, we can compute the Rosseland-mean opacity; using Eq. (12) we find:

$$\langle\kappa\rangle_R \simeq 1.95 \times 10^{-18} \left(\frac{\mathrm{cm}^2}{\mathrm{g}}\right) \left(\frac{m_a}{\mathrm{eV}}\right)^2 \left(\frac{T}{\mathrm{MeV}}\right)^{-1/2} \left(\frac{\rho}{10^{14}\mathrm{gcm}^{-3}}\right) (1 + 8X_n X_p). \tag{15}$$

Of the approximations made in calculating the axion opacity—non-degenerate and non-relativistic nucleons, and constant matrix element squared—the latter is least well justified. Because of the various pion-propagator factors that enter in the matrix element squared, $|\mathcal{M}|^2$ is not constant. The dependence upon the nucleon-momentum transfer enters in the form of the following pion-propagator factors:

$$|\vec{k}|^4/(|\vec{k}|^2 + m_\pi^2)^2, \quad |\vec{l}|^4/(|\vec{l}|^2 + m_\pi^2)^2, \quad |\vec{k}|^2|\vec{l}|^2/(|\vec{k}|^2 + m_\pi^2)(|\vec{l}|^2 + m_\pi^2);$$

see Ref. 9. Here $m_\pi = 135$ MeV is the pion mass, and $k = p_2 - p_4$ and $l = p_2 - p_3$ are the four-momenta transfers in the two types of Feynman diagrams (for details, see Ref. 9). The three-momenta exchanged are $|\vec{k}|^2 \sim |\vec{l}|^2 \sim 3m_N T$; at high temperatures, $T \gg m_\pi^2/3m_N \simeq 6$ MeV, the pion-propagator factors become momentum independent and equal to unity. Deep inside the core, the temperatures are sufficiently high that the pion-propagator factors can be ignored; further out—say near the axion sphere where $T \sim 10$ MeV—the validity of ignoring the pion-propagator factors is less justified.

To be more quantitative about the effect of the pion propagator we have computed the axion-emission rate with a pion-propagator factor included, j_E^{pp}, by multiplying the constant matrix element squared by $|\vec{k}|^4/(|\vec{k}|^2 + m_\pi^2)^2$, and comparing it to the rate computed without the pion-propagator factor—the canonical assumption. (We note that this procedure is not precisely correct, as the pion-propagator factor that occurs in the interference terms in $|\mathcal{M}|^2$ involves both $|\vec{k}|$ and $|\vec{l}|$—see Ref. 9; however, this procedure should give one a pretty good idea of the effect of the pion propagator.)

The ratio of the pion-propagator corrected rate to the uncorrected rate is given by

$$R(\alpha, T) = \frac{\int_0^\infty e^{-x} \left[(x+\alpha)^{1/2} x^{1/2} (1 + 4\epsilon^2/y_+ y_-) - \epsilon \ln(y_+/y_-)\right] dx}{\int_0^\infty e^{-x} (x+\alpha)^{1/2} x^{1/2} dx}, \qquad (16)$$

where $\alpha = E_a/T$, $\epsilon = m_\pi^2/2m_N T$, and $y_\pm = [(x+\alpha)^{1/2} \pm x^{1/2}]^2 + 2\epsilon$. The axion-emission reduction factor R is shown as a function of temperature in Fig. 2 for $E_a/T = 1$, 4, 7, and 10. For $E_a/T = 4$ (a characteristic value for a thermal distribution and for the Rosseland mean) and $T > 10$ MeV, R is greater than about 1/2. Since $\kappa_E \propto j_E$, R is a measure of the reduction in both axion emission and axion opacity due to the effect of pion propagators in the matrix element squared.

It is straightforward to show that R has the following limiting behaviors: $R \to 1 - \mathcal{O}(\epsilon)$ for $\epsilon \to 0$ and $R \to \epsilon^{-2}$ for $\epsilon \gg 1$. Motivated by this we have used the following expression to approximate R:

$$R(\alpha, T) = \frac{1}{1 + a(\alpha)\epsilon + b(\alpha)\epsilon^2}.$$

For $\alpha = E_a/T = 4$, $a = 0.814$ and $b = 0.054$ give the correct limiting behaviours and a fit that is accurate to better than 7% for all values of T. (For reference, $a = 1.027$, $b = 0.0673$ for $\alpha = 3$ and $a = 2.22$, $b = 0.107$ for $\alpha = 1$.) Although the effect of including the pion propagators is small (see end of next Section), we have used the above fit to R for $\alpha = 4$ to correct both $\dot{\varepsilon}_a$ and κ_E for use in the numerical models in Section IV.

III. Axion-Energy Transport

To properly treat the effects of axions upon the cooling of the nascent neutron star associated with SN1987A in the trapping regime ($m_a \gtrsim 10^{-2}$ eV) one must employ the full apparatus of radiative-transfer theory. This is a formidable task, and in light of all the uncertainties—neutron star equation of state, the initial state of the hot neutron star, the imprecision of our "exclusion criterion" based upon the length of the neutrino burst, and especially the question of the existence of the axion itself—we have opted to use an approximation scheme—"leakage"—to describe the transport of axion energy out of the newly born neutron star. In this scheme the local contribution to the net axion volume-emission rate at a given point is the total volume-emission rate at that point, $\dot{\varepsilon}_a$, multiplied by the factor $(1 + k\tau^2)^{-1}$, where τ is the optical depth (integrated Rosseland-mean opacity from the center of the star to infinity) and k is a numerical constant of order unity (which we will argue should be about 0.3). Moreover, as we will show in the next Section, our results are relatively insensitive to the exact value of k. This approach gives the proper result both in the limit that axions freely stream ($\tau \ll 1$) and in the limit that axions are strongly trapped (for the fundamental diffusion mode of a constant density sphere model).

Axion transport in SN 1987A is very similar to photon (radiative) transport in an ordinary star, and so we will adopt the language and machinery that has been developed

for that problem. (For the most part we follow the notation and conventions used in Refs. 13, except we use the axion energy instead of the axion frequency.) The primary quantities of interest are the specific intensity, I_E, and its various moments. The specific intensity describes the flow of energy carried by axions (dE_a) in a particular direction ($\hat{\mathbf{n}}$) through an area ($d\mathbf{A}$) into a solid angle ($d\Omega$) per energy interval ($dE = hd\nu$) per time (dt),

$$I_E = \frac{dE_a}{\cos\theta dA d\Omega dE dt},$$

where θ is the angle between $d\mathbf{A}$ and $\hat{\mathbf{n}}$. The specific intensity I_E is related to the axion phase space density f_a by $I_E = E^3 f_a/h^3c^2$.

The equation of radiative transport (which follows directly from the Boltzmann equation) describes the evolution of I_E and is given by

$$\frac{1}{c}\frac{\partial I_E}{\partial t} + \hat{\mathbf{n}}\cdot\nabla I_E = -\rho\kappa_E(I_E - B_E), \tag{17}$$

where B_E is the previously discussed Planck function (for axions) and only axion absorption and emission have been included (as we have argued in the previous Section, processes involving more than one axion are highly subdominant). Taking the zeroth and first angular moments of this equation it follows that

$$\frac{\partial U_E}{\partial t} + \nabla\cdot\mathbf{F}_E = -\rho\kappa_E c(U_E - 4\pi B_E/c), \tag{18a}$$

$$\frac{1}{c}\frac{\partial \mathbf{F}_E}{\partial t} + c\nabla\cdot\mathcal{P}_E = -\rho\kappa_E\mathbf{F}_E, \tag{18b}$$

where we have defined the following quantities: the differential axion-energy density $U_E = \int I_E d\Omega/c$, the net energy flux $\mathbf{F}_E = \int \hat{\mathbf{n}} I_E d\Omega$, and the differential pressure tensor $\mathcal{P}_E = \int \hat{\mathbf{n}}\hat{\mathbf{n}} I_E d\Omega/c$. (Note that $U_E \equiv d\rho_a/dE$; for consistency with the astrophysical literature we have used U_E in this Section.)

Integrating Eqs. (18a) and (18b) over energy, specializing to spherical symmetry, and neglecting the time variation of the flux $\mathbf{F}_E$ (a valid approximation for times shorter than the diffusion time) we find

$$\frac{\partial U}{\partial t} + \hat{\mathbf{r}}\cdot\frac{\partial \mathbf{F}}{\partial r} = -\rho c\int \kappa_E(U_E - 4\pi B_E/c)dE, \tag{19a}$$

$$\mathbf{F} = -\frac{c}{\rho}\hat{\mathbf{r}}\int \frac{1}{\kappa_E}\frac{\partial P_E}{\partial r}dE \equiv -\frac{c}{\rho\langle\kappa\rangle_R}\frac{\partial P}{\partial r}\hat{\mathbf{r}}, \tag{19b}$$

where a quantity with no subscript E indicates that it has been integrated over energy and $P = \int dE \int I_E \cos^2\theta d\Omega/c$ is the $\hat{\mathbf{r}}\hat{\mathbf{r}}$ component of the pressure. Note that Eq. (19b) is the defining relation for the mean opacity $\langle\kappa\rangle_R$.[13] Substituting Eq. (19b) into Eq. (19a) we obtain

$$\frac{\partial U}{\partial t} - \frac{c}{\rho\langle\kappa\rangle_R}\frac{\partial^2 P}{\partial r^2} = -\rho c\int \kappa_E(U_E - 4\pi B_E/c)dE. \tag{20}$$

If we now use the Eddington approximation,[13] $P \simeq U/3$, which is valid for any nearly isotropic radiation field (i.e., everywhere, except very near the axion sphere) we can rewrite Eq. (20) as

$$\frac{\partial U}{\partial t} - \frac{c}{3\rho\langle\kappa\rangle_R}\frac{\partial^2 U}{\partial r^2} = -\rho c \int \kappa_E (U_E - 4\pi B_E/c) dE. \tag{21}$$

Next we approximate the right-hand side of Eq. (21) by the Rosseland-mean opacity times the rest of the integrand, giving

$$\frac{\partial U}{\partial t} = \frac{c}{3\rho\langle\kappa\rangle_R}\frac{\partial^2 U}{\partial r^2} - \rho c\langle\kappa\rangle_R (U - 4\pi B/c). \tag{22}$$

The physics embodied in Eq. (22) is manifest. The change in the local axion-energy density is driven by two effects: (1) the deviation of the energy density from a black body distribution, $U - 4\pi B/c$; and (2) the diffusion of axions, represented by the $\partial^2 U/\partial r^2$ term. Further, we see that the net rate at which axions are locally removing energy is given by $-c\rho\langle\kappa\rangle_R(U - 4\pi B/c)$: The term proportional to $4\pi B/c$ represents the rate at which axions are being created out of the thermal bath, while the term proportional to U represents the rate at which axions are being absorbed into the thermal bath. Put another way, the net effect of axions is a local heat sink of strength $-\rho c\langle\kappa\rangle_R(U - 4\pi B/c)$.

Now we assume that the spatial derivative in the diffusion term can be approximated by the inverse of a length scale R that is characteristic of the nascent neutron star's radius (i.e., $\partial^2/\partial r^2 \to -1/R^2$) and that the Planck function is independent of time—i.e., that the temperature changes slowly with time—then Eq. (22) can be rewritten as

$$\frac{\partial}{\partial t}\left(U - \frac{4\pi B}{c}\right) = -\left[\frac{1}{\tau_a} + \frac{1}{\tau_D}\right]\left(U - \frac{4\pi B}{c}\right) - \frac{4\pi B/c}{\tau_D}, \tag{23}$$

where $\tau_a = 1/\rho c\langle\kappa\rangle_R$ is the local axion-mean-free time for absorption and $\tau_D = 3\rho\langle\kappa\rangle_R R^2/c$ is the axion-diffusion time. Equation (23) is simple to solve:

$$U - \frac{4\pi B}{c} = -\frac{4\pi B/c}{\tau_D/\tau_a + 1}\left\{1 - \exp\left[-\left(\frac{1}{\tau_D} + \frac{1}{\tau_a}\right)t\right]\right\} \simeq \frac{-4\pi B/c}{\tau_D/\tau_a + 1}. \tag{24a}$$

By using Kirchhoff's law ($\dot{\varepsilon}_a = \rho\int j_E dE = 4\pi\rho\int \kappa_E B_E dE = 4\pi B/c\tau_a$) the steady state solution can be written as

$$\left(U - \frac{4\pi B}{c}\right) = \frac{-\dot{\varepsilon}_a \tau_a}{1 + k\tau^2}. \tag{24b}$$

Here we have replaced $\tau_D/\tau_a = 3\rho^2\langle\kappa\rangle_R^2 R^2$ by $k[\int_0^\infty \rho\langle\kappa\rangle_R dr]^2 \equiv k\tau^2$, where τ is the total optical depth and k is a numerical (diffusion) constant of order unity. The purpose of replacing $3(\rho\langle\kappa\rangle_R R)^2$ by $k\tau^2$ is to better treat the diffusion term, cf. the $\partial^2 U/\partial r^2$ term in Eq. (22), and to allow us to investigate the sensitivity of our scheme to the exact choice for the diffusion scale. In our simple-minded derivation it would follow that $k = 3$; for a

constant-density model it can be shown that $k = 3/\pi^2 \simeq 0.3$ for the fundamental diffusion mode.[14]

Now recall that the net rate at which axions locally remove energy is $-c\rho\langle\kappa\rangle_R(U - 4\pi B/c)$, which from Eqs. (24) is given by

$$-c\rho\langle\kappa\rangle_R\left(U - \frac{4\pi B}{c}\right) = \frac{-\dot{\varepsilon}_a}{1 + k\tau^2}. \tag{25}$$

Equation (25) is the effective heat sink that we will incorporate into our numerical models of the initial cooling of the neutron star associated with SN 1987A. In the limit that $\tau \ll 1$ (freely streaming axions), the effective sink term reduces to the total volume-emission rate $\dot{\varepsilon}_a$ as expected. In the trapping regime ($\tau \gg 1$) the effective sink term is the local axion-volume-emission rate $\dot{\varepsilon}_a$ divided by k times the optical depth squared—the leakage factor. That it should be of this form is easy to see. The time for axions to diffuse out from the center of the star is $\tau_D \sim \tau^2\tau_a$; the energy density in axions is U. One would therefore expect the heat loss due to axions to be U/τ_D; by Kirchhoff's law, cf. Eq. (3), $U \sim \tau_a\dot{\varepsilon}_a$, from which it follows that the heat loss due to axions is $U/\tau_D \sim \dot{\varepsilon}_a/\tau^2$.

IV. Results of Numerical Models

For the purpose of this investigation of the trapped regime, we have focused on a single protoneutron star model, model B from our previous work on the freely streaming regime (Ref. 5, hereafter referred to as BTB). In BTB, we investigated a variety of protoneutron star models, with different equations of state and different masses, and found substantially the same results for all of the models. We feel confident that we can restrict the present studies of the trapping regime to a single model, model B, the model that best reproduces the neutrino observations of SN 1987A. (Model B has a stiff equation of state and the protoneutron star mass starts at 1.3 $M_\odot$ and increases by accretion to about 1.5 $M_\odot$.)

For the most part we will follow the approach of BTB. To briefly remind the reader of the strategy of the previous work, we first computed the neutrino flux from a numerical simulation of the cooling of the nascent neutron star that included freely streaming axion emission. From this flux and the response characteristics of the KII and IMB water Cherenkov detectors we computed the number of $\bar{\nu}_e$-capture events expected for each detector, N, and the time required for the expected number of events to reach 90% of its asymptotic value, $\Delta t_{90\%}$, again for each detector. In addition, we computed the total energy carried off by axions (E_a) and by neutrinos (E_ν).

Both the energy carried off by neutrinos and the number of capture events were only mildly sensitive to the effects of axion emission; we found that the most sensitive indicator of axion emission was $\Delta t_{90\%}$. As the assumed axion mass was increased to about 10^{-3} eV, the neutrino burst duration dropped precipitously to less than about 1 sec for both detectors, in contrast to the observed burst durations of about 12 sec (KII)[17] and about 6 sec (IMB);[18] see Fig. 3. On this basis, in BTB we concluded that the KII and IMB

data excluded an axion more massive than about 10^{-3} eV (at least in the freely streaming regime).

However, as we have discussed earlier, for an axion mass greater than about 10^{-2} eV axions, once produced, do not simply stream out. Rather, because their "optical" depth, $\tau = \int_0^\infty dr/\lambda_a$, exceeds unity, an axion emitted deep inside the neutron star is likely to be reabsorbed before it can escape. Axions are said to become trapped, and above the trapping mass the axion luminosity begins to drop significantly; see Fig. 1. At a sufficiently large value of the axion mass, estimated in Ref. 3 to be about 2 eV, axion emission has no significant effect on the neutrino-burst duration. Therefore, there is only an interval of axion masses—very roughly between 10^{-3} eV and about 1 eV—that is excluded by the supernova, and it is the high-mass boundary of this interval that is the subject of this paper.

We used the same general-relativistic stellar-evolution code employed in BTB, discussed in detail in Refs. 15 and 16. Numerical simulations of the initial cooling phase (first 12 to 20 sec) of a hot neutron star that incorporate the axion-heat sink given in Eq. (25) (and mutiplied by the pion-propagator reduction factor $R(\alpha = 4, T)$, cf. Eq. (16) and below) were performed for axion masses from 0.01 eV to 10 eV and, to explore the sensitivity of these results to the diffusion constant k, for values $k = 0.1$, 0.3, and 1. In all, 21 protoneutron star cooling models were run. For each model we computed E_a, E_ν, N and $\Delta t_{90\%}$ for both detectors, and the total Rosseland-mean opacity integrated from the center of the star outward at the final time step (usually $t = 20$ sec). In addition, at times of 0.05 sec, 0.1 sec, 0.5 sec, 1.0 sec, 5.0 sec, 10 sec, and 20 sec we computed the average axion energy of axions emitted from the axion sphere (the bulk of the axion luminosity should come from the axion sphere). Our results are given in Tables I and II and illustrated in Figs. 1 and 3-8. In addition, both for completeness and comparison, in Figs. 1, 3, and 5 we have shown the results of our previous work for the freely streaming regime.

The behavior of our best barometer for axion emission—the burst duration $\Delta t_{90\%}$—is shown in Fig. 3 for axion masses from 10^{-4} eV to 10 eV, spanning both the freely streaming and trapping regimes. One can clearly see the effect of axion emission on the neutrino burst: As the axion mass is increased to about 10^{-3} eV the burst duration drops precipitously due to the effect of axion emission; at a mass of about 10^{-2} eV, where trapping sets in, the burst duration has reached its minimum value and begins to increase with increasing axion mass; and finally, at an axion mass of about 0.3 eV or so, trapping has reduced the effects of axion emission on the burst duration to a negligible level once again. Also note that axion emission reduces the burst duration for both KII and IMB by about the same factor.

To remind the reader of the physical origin of the precipitous drop in burst duration, first found in BTB, it traces to the fact that there are two distinct phases of neutrino emission. The first phase, lasting of order 1 sec, is powered by the heat in the outer

mantle and residual accretion; the second phase, lasting of order many seconds, is powered by the outward diffusion of the heat trapped in the inner core. The first phase is rapid because the timescales for neutrino diffusion out of the low density outer mantle and for residual accretion are both short ($\lesssim 1$ sec). The second phase lasts much longer because the timescale for diffusion of neutrinos from the inner core is long, of order many seconds. Axion emission tends to deplete the heat trapped in the inner core that powers the second phase of neutrino emission by providing another means of transporting heat out of the inner core. By so doing, axion emission can drastically shorten the duration of the neutrino burst.

It is expected that the trapping sets in at an axion mass of about 10^{-2} eV; in Table I we show the total axion opacity ($\tau = \int_0^\infty dr/\lambda_a$) at the final time step. For an axion mass of 10^{-2} eV, $\tau \sim 0.2$, and τ increases to about 1.7 for an axion mass of 3×10^{-2} eV. We see that axion trapping sets in very close to the axion mass where it was expected to set in: about 2×10^{-2} eV.[3] We should also mention that our present results for an axion mass of 10^{-2} eV agree quite well with our previous results (BTB), where we assumed that axions were freely streaming.

As in the freely streaming regime, the number of capture events (see Fig. 5) and the energy carried off in neutrinos (see Fig. 1) are much less sensitive indicators of axion emission: At a mass of about 10^{-2} eV the expected number of events falls by less than a factor of 2, and at most axions carry away as much energy as the neutrinos do. Again, this is simple to understand: Axion emission does not directly suppress neutrino emission; rather, axions tap the same source of energy as do neutrinos and thus axion cooling serves only to shorten the cooling time.

The total energy carried away by axions is shown in Figs. 1 and 6. In the regimes where axions are a minor heat sink, axion masses much smaller or much greater than 10^{-2} eV, one can, for purposes of understanding how E_a scales, ignore the back reaction of axions on the cooling of the neutron star. Doing so, in the low mass regime one expects the energy carried off by axions should vary as m_a^2 since the axion luminosity is proportional to $\dot{\epsilon}_a$ which varies as m_a^2. In the high mass regime, the situation is more complicated because of axion trapping. However, one expects the axion luminosity to vary as the temperature of the axion sphere to the fourth power, and in Ref. 3 it was estimated that the temperature of the axion sphere should vary as $m_a^{-4/11}$; this implies that the energy carried off by axions should vary as $m_a^{-16/11}$ in the large mass limit. Both of these scalings are roughly consistent with our numerical results for the temperature of the axion sphere and the energy carried away by axions; see Figs. 1, 6, and 8.

It may be of some interest to know the average energy of the axions emitted by a nascent neutron star in the trapping regime, e.g., if one envisions nascent neutron stars as an intense source of axions that might be detected by other means.[19] In Table II and Figs. 7 and 8 we have shown the average energy of an axion emitted from the axion sphere at times of 0.05 sec, 0.1 sec, 0.5 sec, 1.0 sec, 5.0 sec, 10 sec, and 20 sec. These energies were

obtained as follows. Axions emitted from the axion sphere were assumed to have a thermal distribution with a temperature equal to that of the nuclear matter, and the axion sphere was located by finding the surface beyond which the integrated opacity equals 2/3, i.e., $\int_{R_a}^{\infty} \rho \langle \kappa \rangle_R dr = 2/3$. The average axion energy was then computed to be $2.701 T_a/(1+z)$, where $(1+z)$ is the gravitational red shift from the axion sphere to infinity. (The total energies carried off by axions and neutrinos discussed earlier were red shifted in the same way.) One can see that the temperature of the axion sphere typically drops rapidly during the first 0.5 sec and then slowly falls thereafter. (For axion masses of 0.03 eV and 0.1 eV, the axion sphere temperature increases initially.) To estimate the average axion energy for the integrated luminosity, the value at a time of around 1 sec is probably the best indicator; this is shown in Fig. 8, as well as its dependence upon k.

As we have discussed in the previous Section, the preferred value of the diffusion constant k is 0.3; however, we have run models with $k = 0.1$ and 1 also. To understand the dependence of our results upon the diffusion constant k, recall that the k dependence enters directly only through the effective axion-heat sink which is given by $\dot{\varepsilon}_a/(1+k\tau^2)$. For small axion masses, $m_a \ll 10^{-2}$ eV, where $\tau \ll 1$, the k dependence disappears. For large axion masses, the effective axion-energy sink is proportional to k^{-1}; thus in the limit that axions are trapped and have little back reaction on the cooling of the neutron star one would expect that the energy carried away by axions should scale as k^{-1}. This is seen in Fig. 6 and in Table I. The dependence of the temperature of the axion sphere is less severe, as one would expect. While the dependence of $\Delta t_{90\%}$ upon k is significant, cf. Fig. 4, our exclusion criterion is not so sharp, nor are other uncertainties so small, that the k dependence warrants more careful calculations of axion transport at this time. In fact, if one had a fixed criterion in mind, e.g., KII burst of shorter than 2 sec is unacceptably short, the upper mass boundary derived would vary by only about a factor of 3 in going from the $k = 1$ (smallest upper mass boundary) to $k = 0.1$ (largest upper mass boundary) results. For an axion mass of 0.3 eV, the duration of the expected KII burst would be about 3 sec and for IMB about 1 sec for $k = 0.1$—and even larger for $k = 0.3$ or 1. For an axion mass of 1 eV, the duration of the expected KII burst would be about 6 sec and for IMB about 3 sec for $k = 0.1$. Based upon $\Delta t_{90\%}$, the most sensitive indicator of axion emission, an axion mass of 0.3 eV or larger would seem to be consistent with the KII and IMB data. To be very conservative, one might insist that the axion should be greater than about 1 eV.

Finally, we briefly comment upon the inclusion of the pion-propagator correction factor $R(\alpha, T)$. In general, its effect upon of our results was small (typically 10% to 20%) and would not have affected any of our conclusions (had we not included it). As expected, the effect of including this correction was most significant for large axion masses, for which the temperature of the axion sphere is the smallest (recall that $T_a \propto m_a^{-4/11}$). Based upon the very small effect of including this correction on our $m_a = 10^{-2}$ eV results, we feel confident that not including the pion-propagator in our previous work[5] was a well justified

approximation. For the interested reader $k = 0.3$ results obtained without the correction factor R have been included at the end of Table I.

V. Concluding Remarks

The existence of an axion of mass in the range 10^{-3} eV to about 1 eV would have had a significant effect upon the cooling of the nascent neutron star associated with SN 1987A (and upon other nascent neutron stars). For such a mass, axions would carry away a significant fraction of the energy and would significantly accelerate the cooling process. We have now investigated in detail the effect of axion cooling both in the freely streaming regime ($m_a \lesssim 10^{-2}$ eV) and in the trapping regime ($m_a \gtrsim 10^{-2}$ eV). Based upon the duration of the expected neutrino bursts calculated in our axion-cooled models, an axion mass in the interval 10^{-3} eV to 0.3 eV seems to be excluded. The upper mass boundary is slightly smaller than that estimated in Ref. 3. Therefore, the axion mass window around a few eV opens up, and is now 0.3 eV to 5 eV (hadronic axions only). The portion of this window from about 2 eV to 5 eV will be explored by a search for the decays of relic cosmological axions which will be carried out at Kitt Peak this year.[6] If that search is unsuccessful, it will still leave open a portion of the multi-eV axion-mass window, from about 0.3 eV to 2 eV. That portion of the window is accessible to an experiment that has been proposed to search for axions emitted by the Sun.[7] It is also possible that this mass region could be explored if a supernova explosion occurred within our own galaxy, e.g., by more closely examining the neutrino signal (provided that many more events are detected) or by other means such as gamma-ray observations.[19]

As we emphasized earlier in this paper and in BTB, our results, which are expressed in terms of the axion mass, actually depend upon the values of the axion-nucleon couplings; for definiteness we have assumed that $c_n = c_p = \frac{1}{2}$ where $g_{an} = c_n m_N/(f_a/N)$ and $g_{ap} = c_p m_N/(f_a/N)$. The dimensionless axion-nucleon couplings c_n and c_p depend upon the PQ charges of the quark species and the quark-distribution functions; the couplings are discussed in some detail in Refs. 20. Both mass boundaries for the excluded mass region scale with the inverse of the axion-nucleon couplings; that is, doubling c_n and c_p would decrease both the upper and lower mass boundaries by a factor of two. (Of course, the rescaling of the boundaries of the excluded region is more difficult if c_n and c_p do not change in the same way; however, one could probably still estimate the change.)

Finally, we should mention the uncertainties inherent in our axion mass constraint. To begin with, there are the uncertainties associated with our numerical cooling models—equation of state, neutron star mass, amount of residual accretion, leakage approximation of axion transport, and our exclusion criterion for the duration of the neutrino burst. While these uncertainties could amount to a factor of a two or so in the mass boundary, additional uncertainty beyond that does not seem likely. The uncertainty in the axion-emission rate and opacity are a different matter. Deep in the core of the nascent neutron

star the densities certainly reach several times that of nuclear matter; there may be high-density effects, nuclear many-body effects—or even an exotic form of matter at the core, e.g., quark matter or a pion condensate—that could significantly affect the axion emission rate or opacity. The high-density effects have discussed in Ref. 11 and do not seem likely to affect either the axion luminosity or opacity significantly. In any case, the uncertainties associated with the high densities at the core of the neutron star would probably only affect the low mass boundary, as only in the freely streaming regime does most of the axion luminosity come from the core. In the trapping regime, most of the axion luminosity comes from the axion sphere, which around the upper mass boundary is near the neutrino sphere ($T \sim 10$ MeV and $\rho \sim 10^{12}$ g cm^{-3}).

Almost since its conception, it has been realized that the axion could significantly affect the cooling of stars of all kinds. Because the evolutionary timescales for most stars are measured in millions, if not billions, of years, the astrophysical arguments based upon stellar evolution that have been used to constrain the axion mass have necessarily been indirect.[2] The lone exception is SN 1987A; here the 19 neutrino events detected by KII and IMB provide the complete cooling history of the newly born neutron star. Based upon that cooling record an axion mass in the range 10^{-3} eV to 0.3 eV is excluded. Not only is this constraint the most stringent astrophysical constraint to the axion mass, but the directness of the argument is most pleasing.

Acknowledgments

This work was supported in part by the DOE (at Chicago and Fermilab), the NASA through NAGW-1340 (at Fermilab) and through MTR's GSRP (at Chicago), and by the NSF through Grants No. AST 87-14176 and 89-14346 (at Arizona).

References

1. R.D. Peccei and H.R. Quinn, *Phys. Rev. Lett.* **38**, 1440 (1977); F. Wilczek, *Phys. Rev. Lett.* **40**, 279 (1978); S. Weinberg, *Phys. Rev. Lett.* **48**, 223 (1978). The "invisible axion" is of two generic types: DFS, first discussed by M. Dine, W. Fischler, and M. Srednicki, *Phys. Lett. B* **104**, 199 (1981), and A. Zhitnitsky, *Yad. Fiz.* **31**, 497 (1980) [*Sov. J. Nucl. Phys.* **31**, 260 (1980)]; and hadronic, first discussed by J.-E. Kim, *Phys. Rev. Lett.* **43**, 103 (1979), and M. Shifman, A. Vainshtein, and V. Zakharov, *Nucl. Phys.* **B166**, 493 (1980). For a recent review of the axion see R.D. Peccei, in *CP Violation*, ed. C. Jarlskog (WSPC, Singapore, 1989).
2. See, e.g., M.S. Turner, in *Proc. of the Workshop on Cosmic Axions*, eds. C. Jones and A. Melissinos (WSPC, Singapore, 1990), and *Phys. Rept.*, in press (1990); or G.G. Raffelt, *Phys. Rept.*, in press (1991).
3. M.S. Turner, *Phys. Rev. Lett.* **60**, 1797 (1988).

4. N. Iwamoto, *Phys. Rev. Lett.* **53**, 1198 (1984); A. Pantziris and K. Kang, *Phys. Rev. D* **33**, 3509 (1986); J.E. Ellis and K.A. Olive, *Phys. Lett. B* **193**, 525 (1987); R. Mayle, et al., *Phys. Lett. B* **203**, 188 (1988); *ibid* **219B**, 515 (1989); G.G. Raffelt and D. Seckel, *Phys. Rev. Lett.* **60**, 1793 (1988); M.S. Turner, *ibid* **60**, 1797 (1988); A. Burrows, M.S. Turner and R.P. Brinkmann, *Phys. Rev. D* **39**, 1020 (1989); R.P. Brinkmann and M.S. Turner, *Phys. Rev. D* **38**, 2338 (1988); M.S. Turner, H.-S. Kang, and G. Steigman, *Phys. Rev. D* **40**, 299 (1989); K. Choi, K. Kang, and J.-E. Kim, *Phys. Rev. Lett.* **62**, 849 (1989); N. Iwamoto, *Phys. Rev. D* **39**, 2120 (1989); M. Carena and R.D. Peccei, *Phys. Rev. D* **40**, 652 (1989); T. Hatsuda and M. Yoshimura, *Phys. Lett. B* **203**, 469 (1988); T.E.O. Ericson and J.-F. Mathiot, *Phys. Lett. B* **219**, 515 (1989); N. Ishizuka and M. Yoshimura, Tohoku Univ. preprint TU-349 (1989).
5. A. Burrows, M.S. Turner, and R.P. Brinkmann, *Phys. Rev. D* **39**, 1020 (1989).
6. T. Kephart and T. Weiler, *Phys. Rev. Lett.* **58**, 171 (1987); M.S. Turner, *Phys. Rev. Lett.* **59**, 2489 (1987); M. Bershady, M.T. Ressell, and M.S. Turner, Kitt Peak Observing Proposal (1989), approved for May 1990.
7. K. van Bibber, P.M. Mc Intyre, D.E. Morris, and G.G. Raffelt, *Phys. Rev. D* **39**, 2089 (1989).
8. See, e.g., D. Kaplan, *Nucl. Phys.* **B260**, 215 (1985); M. Srednicki, *Nucl. Phys.* **B260**, 689 (1985); P. Sikivie, in *Cosmology and Particle Physics*, eds. E. Alvarez et al. (WSPC, Singapore, 1986); R. Mayle, et al., *Phys. Lett. B* **219**, 515 (1989); or Ref. 3. The conventions and notation here follow Ref. 3.
9. R.P. Brinkmann and M.S. Turner, *Phys. Rev. D* **38**, 2338 (1988); in the degenerate regime the matrix element and phase-space have also been evaluated by N. Iwamoto, *Phys. Rev. Lett.* **53**, 1198 (1984). The fully relativistic matrix element and phase-space integrations have been carried out by M.S. Turner, H.-S. Kang, and G. Steigman, *Phys. Rev. D* **40**, 299 (1989), and by N. Ishizuka and M. Yoshimura, Tohoku Univ. preprint TU-349 (1989).
10. N. Ishizuka and M. Yoshimura, Tohuku Univ. preprint TU-349 (1989). Since they calculate λ_a in the completely degenerate limit, their work is complementary to the present work and not applicable for the initial stages of cooling since the conditions are nondegenerate.
11. M.S. Turner, H. Kang, and G. Steigman, *Phys. Rev. D* **40**, 299 (1989); also see, Ishizuka and Yoshimura in Ref. 10.
12. I.S. Gradshteyn and I.M. Ryzhik, *Table of Integrals, Series, and Products* (Academic Press, London, 1980), p. 319.
13. See, e.g., G.W. Collins, *The Fundamentals of Stellar Atomspheres* (W.H. Freeman & Co., New York, 1989), pp. 227-251, 303-307; S.L. Shapiro and S.A. Teukolsky, *Black Holes, White Dwarfs, and Neutron Stars* (J. Wiley & Sons, New York, 1983); D. Mihalas, *Stellar Atmospheres* (W.H. Freeman, San Francisco, 1970), pp. 1-41; D. Mihalas

and B.W. Mihalas, *Foundations of Radiation Hydrodynamics* (Oxford Univ. Press, New York, 1984).

14. More precisely, the constant k is in essence a geometric factor. Axions emitted by a shell at radius r diffuse in all directions—from radially outward where the opacity "seen" by axions is only $\int_r^\infty dr/\lambda_a$ to radially inward where the opacity "seen" by axions is $2\int_r^\infty dr/\lambda_a + \int_r^\infty dr/\lambda_a$. By replacing τ_D/τ_a by $k[\int_0^\infty dr/\lambda_a]^2$, k takes into account the average opacity seen over all directions. For a constant density model and the fundamental mode of diffusion one can show that $k = 3/\pi^2$; see, e.g., G.B. Rybicki and A.P. Lightman, *Radiative Processes in Astrophysics* (J. Wiley & Sons, New York, 1979). In using a "leakage" approximation scheme for a nonuniform density model selecting the proper value for k is a bit of an art. Remarkably, in most circumstances the value of k that best reproduces the results of a proper treatment of energy transport does not differ much from $k = 0.3$. In the context of neutrino transport in neutron stars the leakage approximation scheme has been studied extensively by K. Van Riper and J.M. Lattimer, *Astrophys. J.* **249**, 270 (1981). In addition, one might want to compare the results of neutrino transport in neutron stars using a leakage scheme (A. Burrows and J.M. Lattimer, *Astrophys. J.* **299**, L19 (1985)) with those using full neutrino transport (S.W. Bruenn, *Astrophys. J. Suppl.* **58**, 771 (1986)). Given the relative insensitivity of our results to k and the previous experience with the leakage approximation, we feel confident that our treatment of axion transport here is more than adequate for present purposes.
15. A. Burrows and J.M. Lattimer, *Astrophys. J.* **307**, 178 (1986).
16. A. Burrows, *Astrophys. J.* **334**, 891 (1988).
17. R.M. Bionta, et al., *Phys. Rev. Lett.* **58**, 1494 (1987).
18. K. Hirata, et al., *Phys. Rev. Lett.* **58**, 1490 (1987).
19. E.W. Kolb and M.S. Turner, *Phys. Rev. Lett.* **62**, 509 (1989).
20. M.S. Turner, *Phys. Rept.*, in press (1990); G.G. Raffelt, *Phys. Rept.*, in press (1991); Ref. 3; R. Mayle, et al., *Phys. Lett. B* **219**, 515 (1989).

FIGURE CAPTIONS

Fig. 1. Total energy carried off from SN 1987A by axions (solid curve) and neutrinos (broken curve) as a function of axion mass. The results for $m_a \leq 10^{-2}$ eV were taken from our previous work[5] (model B). The results for $m_a \geq 10^{-2}$ eV are from the present work (with $k = 0.3$). In agreement with simple agruments, the energy carried off by axions scales as m_a^2 for small axion masses and as $m_a^{-1.6}$ for large axion masses.

Fig. 2. The pion-propagator reduction factor, $R(\alpha, T)$, as a function of temperature for $\alpha = E_a/T = 1$, 4, 7, and 10. The pion-propagator reduction factor is the factor by which the pion propagators in the matrix element for nucleon-nucleon, axion bremsstrahlung reduce both the axion-emission rate and opacity relative to the approximation where the pion-propagator factors are ignored, cf. Eq. (16).

Fig. 3. The expected neutrino-burst duration, $\Delta t_{90\%}$, in the KII and IMB detectors for axion-cooled nascent neutron star models as a function of axion mass. The results for $m_a \leq 10^{-2}$ eV were taken from our previous work[5] (model B). The results for $m_a \geq 10^{-2}$ eV are from the present work (with $k = 0.3$). The quantity $\Delta t_{90\%}$ is the time required for the expected number of neutrino events to achieve 90% of its asymptotic value. Based upon the expected duration of the neutrino burst, axion masses in the interval 10^{-3} eV to 0.3 eV are excluded by the KII and IMB data. Note that the burst duration in both detectors is reduced by about the same factor.

Fig. 4. Same as Fig. 3, except that only the results of the present work are shown and for three values of the diffusion constant k (0.1, 0.3, and 1). Note that as one enters the freely streaming regime ($m_a = 10^{-2}$ eV) the k dependence disappears, as it should.

Fig. 5. The expected number of neutrino-capture events for the KII and IMB detectors for our axion-cooled neutron star models as a function of axion mass. The results for $m_a \leq 10^{-2}$ eV were taken from our previous work[5] (model B). The results for $m_a \geq 10^{-2}$ eV are from the present work. As described in Section IV, the expected number of events is relatively insensitive to the effect of axion cooling. Note that as one enters the freely streaming regime ($m_a = 10^{-2}$ eV) the k dependence disappears, as it should.

Fig. 6. The energy carried off by axions as a function of axion mass for three values of the diffusion constant k (0.1, 0.3, and 1). Note that as one enters the freely streaming regime ($m_a = 10^{-2}$ eV) the k dependence disappears, as it should. (Same as Fig. 1, except only the results of the present work are illustrated.)

Fig. 7. The average energy of an axion emitted from the axion sphere as a function of time for axion masses of 0.03 eV, 0.1 eV, 0.3 eV, 1 eV, 2 eV, 3 eV, 5 eV, and 10 eV (with diffusion constant $k = 0.3$).

Fig. 8. The average energy of an axion emitted from the axion sphere as a function of axion mass at time 1.0 sec and for diffusion constant $k = 0.1$, 0.3, and 1.

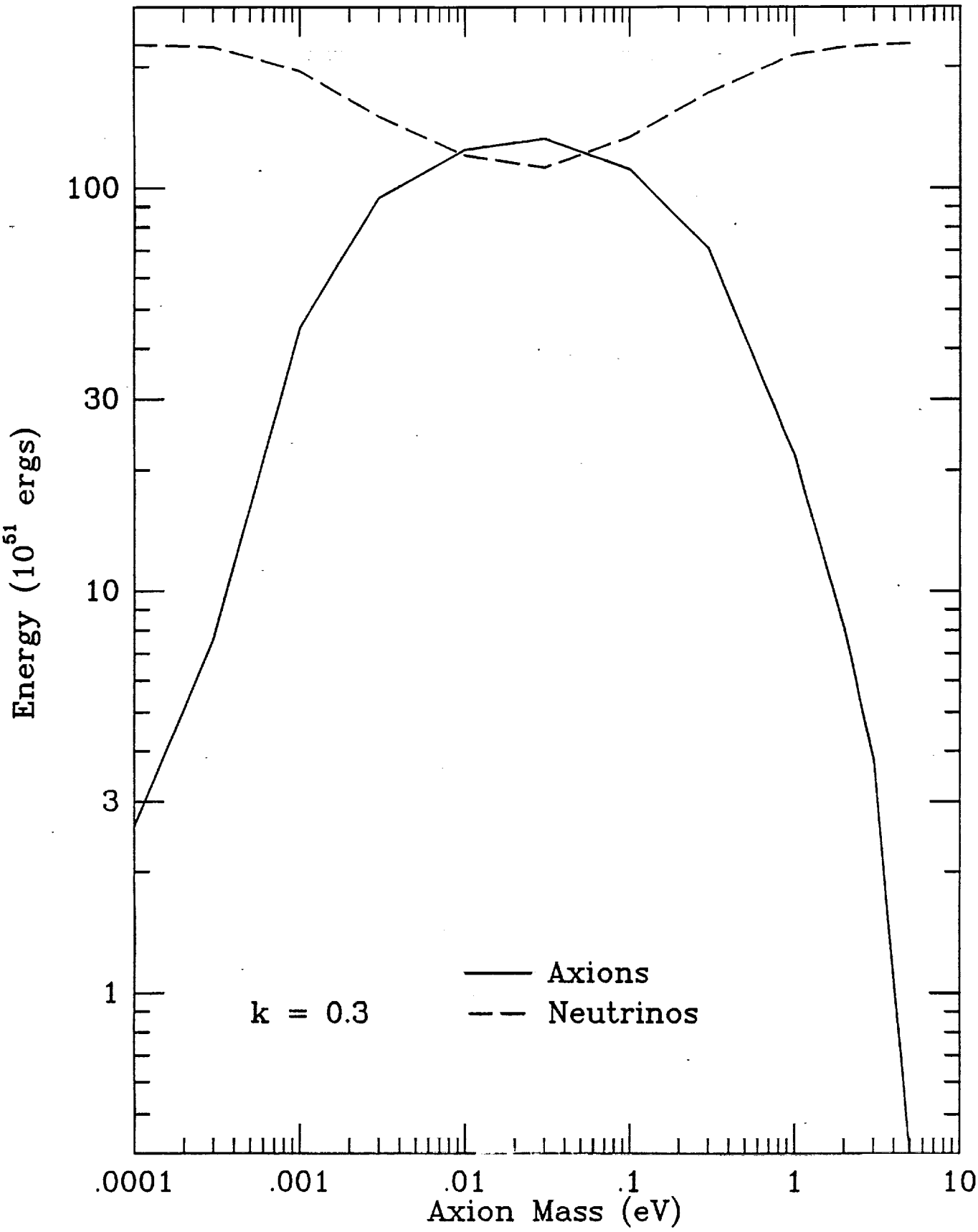
100
30
10
3
1
Energy (10^{51} ergs)
k = 0.3
Axions
Neutrinos
.0001
.001
.01
.1
1
10
Axion Mass (eV)

- FIG 1 -

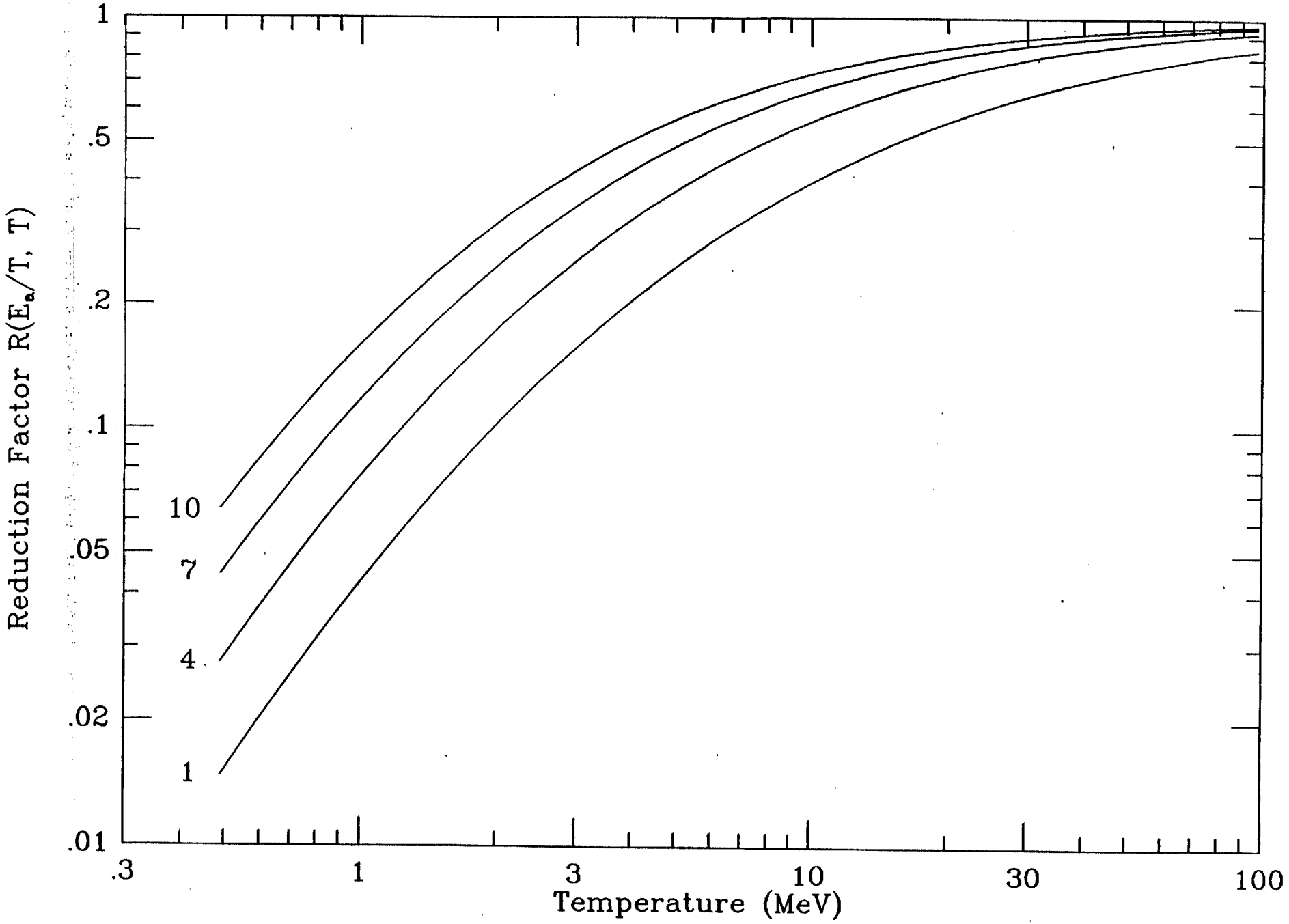
1
.5
.2
.1
.05
.02
.01
Reduction Factor R(E_a/T, T)
10
7
4
1
.3
1
3
10
30
100
Temperature (MeV)

- FIG 2 -

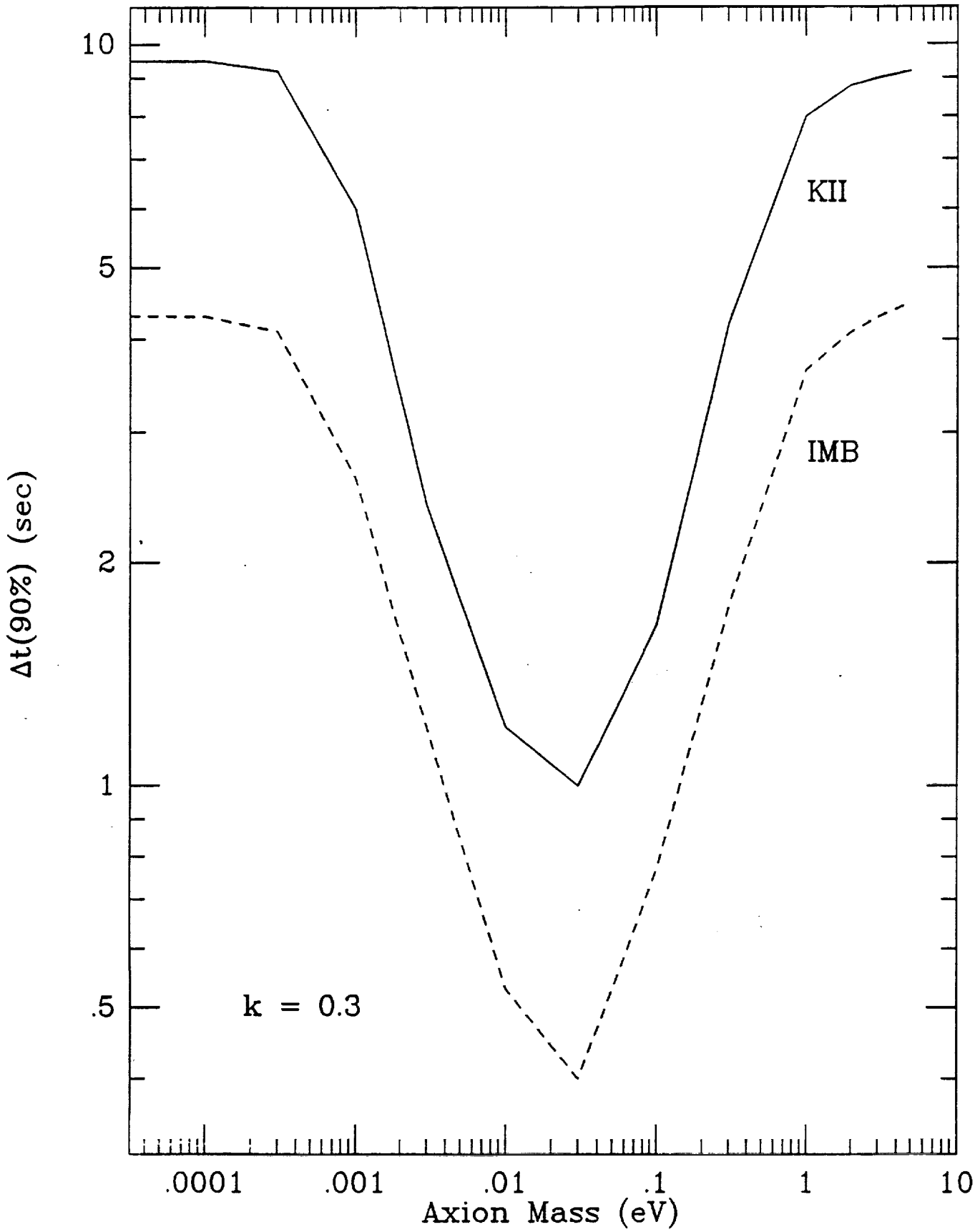

– FIG 3 –

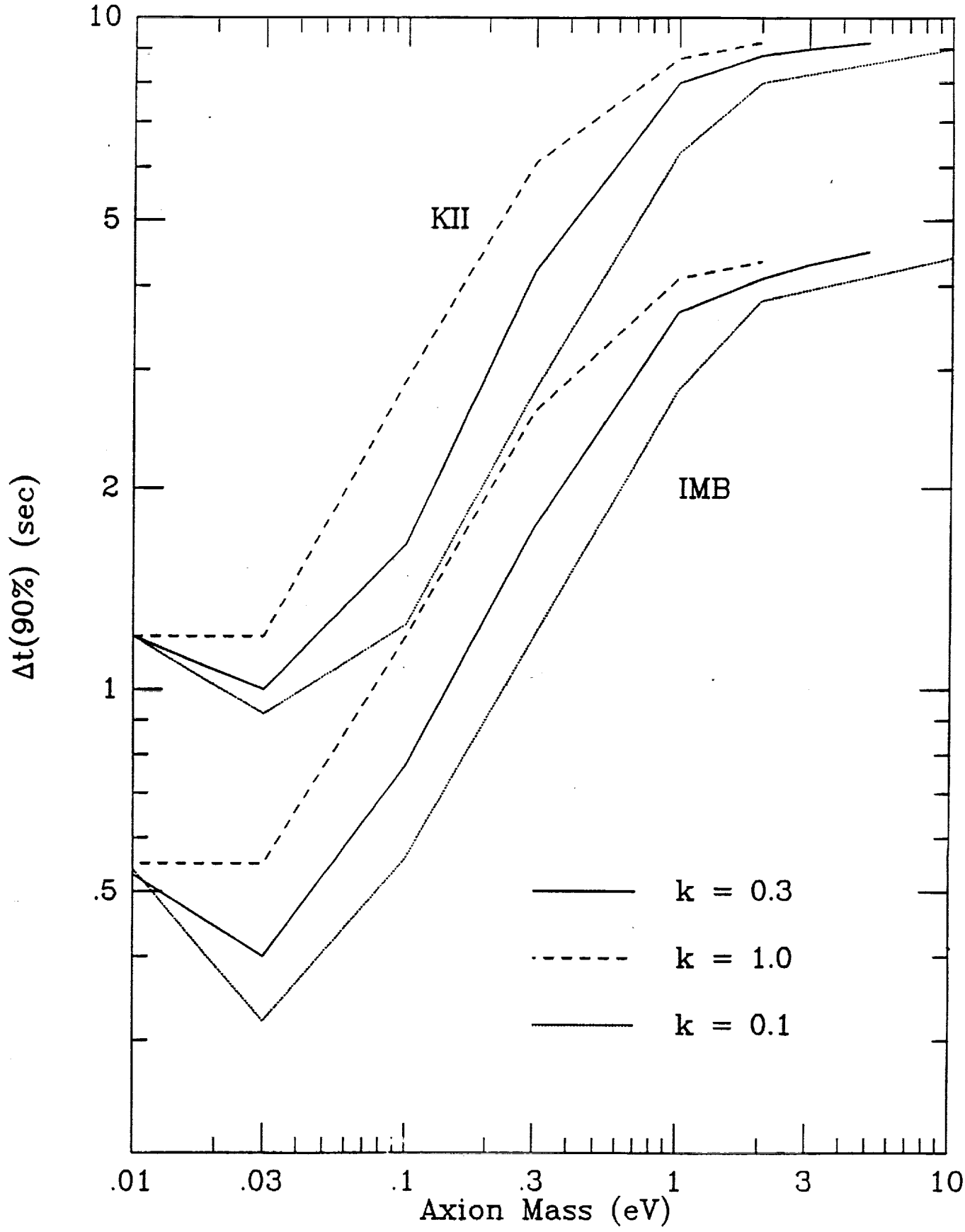

- FIG 4 -

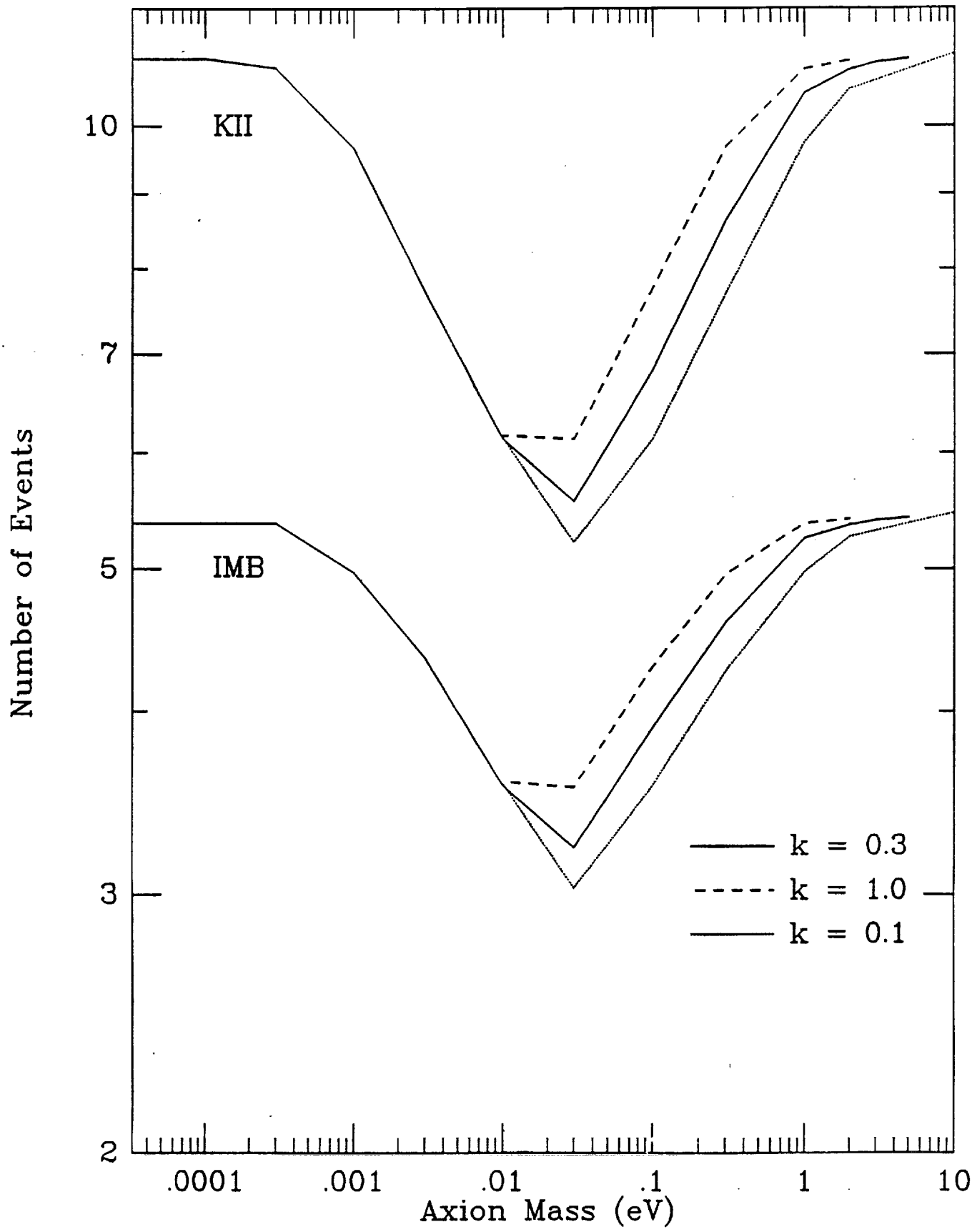
KII
IMB
10
7
5
3
2
Number of Events
.0001
.001
.01
.1
1
10
Axion Mass (eV)
k = 0.3
k = 1.0
k = 0.1

- FIG 5 -

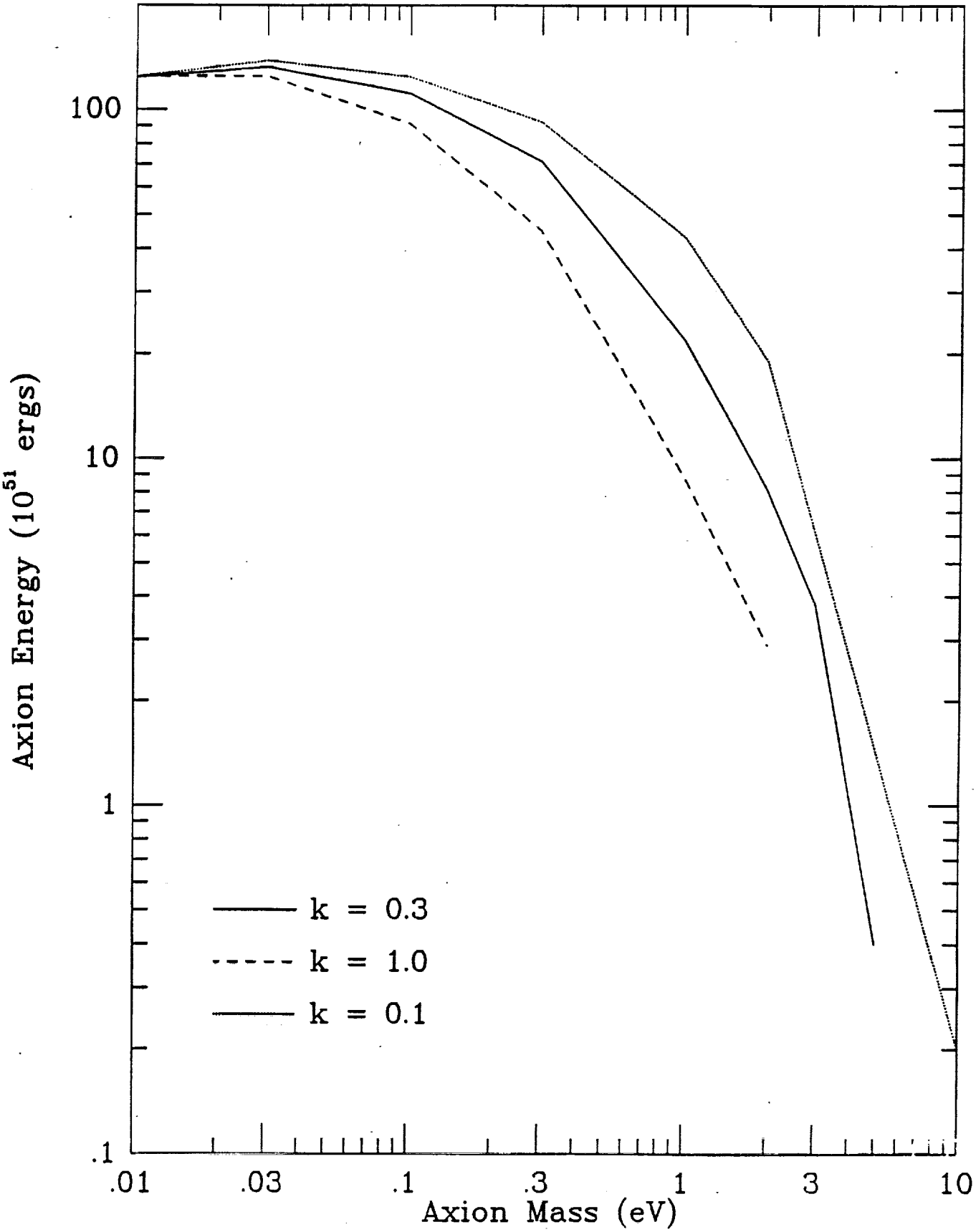
100
10
1
.1
Axion Energy (10^{51} ergs)
.01
.03
.1
.3
1
3
10
Axion Mass (eV)
k = 0.3
k = 1.0
k = 0.1

- FIG 6 -

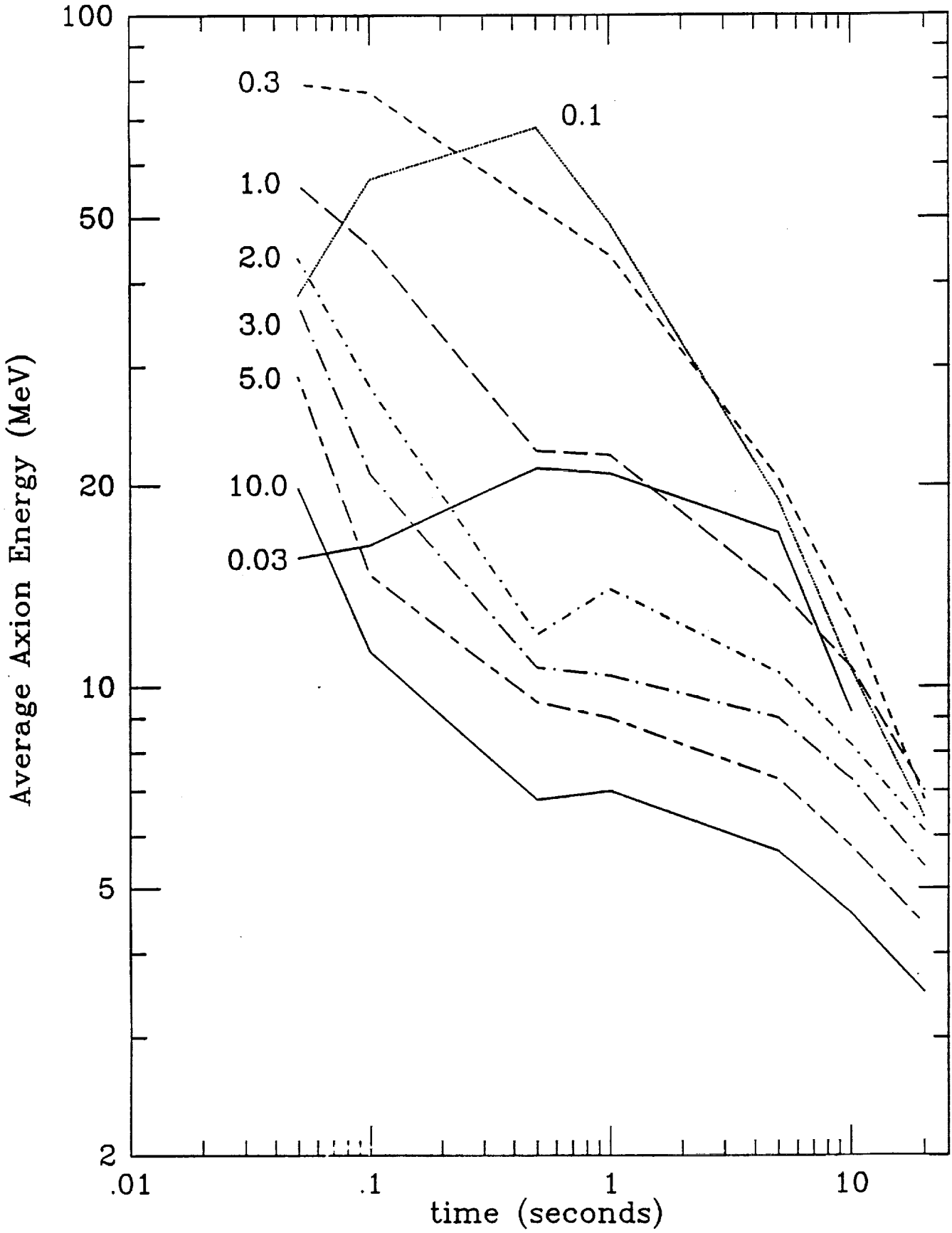
100
50
20
10
5
2
Average Axion Energy (MeV)
0.3
0.1
1.0
2.0
3.0
5.0
10.0
0.03
.01
.1
1
10
time (seconds)

-FIG 7-

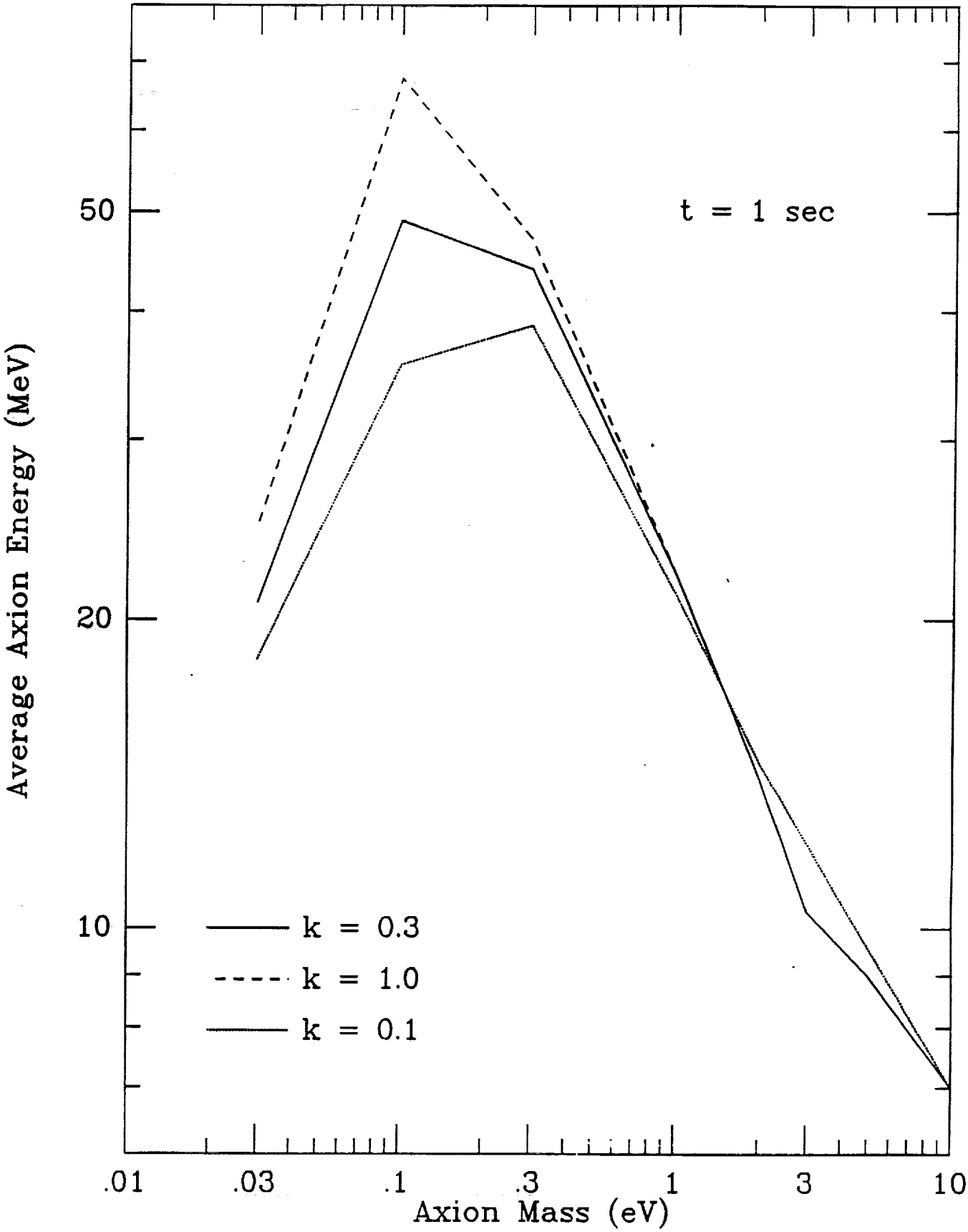
t = 1 sec
Average Axion Energy (MeV)
50
20
10
k = 0.3
k = 1.0
k = 0.1
.01
.03
.1
.3
1
3
10
Axion Mass (eV)

- FIG 8 -

Table I. Summary of axion-cooled nascent neutron star models for $k = 0.1$, 0.3, and 1, and axion masses from 10^{-2} eV to 10 eV. The quantity τ is the total axion opacity ($= \int_0^\infty dr/\lambda_a$) at the final time step. The last set of results for $k = 0.3$ were obtained without including the correction factor for the pion propagators.

Axion mass (eV)	Number of events KII	IMB	Energy (10^{51}ergs) Axions	$\nu\bar{\nu}$	Δt(90%) (sec) KII	IMB	Duration of calculation (sec)	Optical depth, τ
			k	**=**	**0.3**			
0.01	6.13	3.56	124.3	120.4	1.2	0.53	15	0.195
0.03	5.56	3.23	132.9	112.4	1.0	0.4	15	1.68
0.1	6.83	3.90	111.3	134.0	1.65	0.77	20	19.0
0.3	8.62	4.60	71.1	172.4	4.2	1.75	20	189.0
1.0	10.53	5.25	21.8	214.6	8.0	3.65	20	2.06×10^3
2.0	10.92	5.36	8.1	223.8	8.8	4.1	20	7.87×10^3
3.0	11.05	5.40	3.8	226.4	9.0	4.3	20	1.75×10^4
5.0	11.11	5.42	0.4	227.8	9.2	4.5	20	4.86×10^4
			k	**=**	**0.1**			
0.01	6.14	3.57	124.6	121.7	1.2	0.54	12	0.187
0.03	5.21	3.03	138.7	107.5	0.92	0.32	15	1.69
0.1	6.13	3.56	124.2	120.5	1.25	0.56	15	19.1
0.3	7.69	4.26	92.3	151.7	2.8	1.2	20	178.0
1.0	9.74	4.98	43.0	197.8	6.3	2.8	20	2.11×10^3
2.0	10.60	5.26	19.0	216.8	8.0	3.8	20	8.16×10^3
10.0	11.19	5.46	0.2	228.9	9.0	4.4	20	1.93×10^5
			k	**=**	**1.0**			
0.01	6.16	3.58	124.8	120.9	1.2	0.55	15	0.195
0.03	6.13	3.55	125.0	120.3	1.2	0.55	15	1.73
0.1	7.76	4.29	91.1	151.2	2.9	1.2	15	21.2
0.3	9.67	4.96	45.0	196.1	6.1	2.6	20	191.0
1.0	10.93	5.37	8.8	223.7	8.7	4.1	20	1.97×10^3
2.0	11.08	5.41	2.9	227.0	9.2	4.35	20	7.76×10^3
			k	**=**	**0.3**			
0.01	5.96	3.48	127.4	117.3	1.1	0.49	15	0.64
0.03	5.98	3.49	128.9	117.3	1.1	0.52	15	5.83
0.1	7.41	4.18	100.7	145.0	2.2	1.0	20	60.4
0.3	9.23	4.84	57.2	185.4	5.1	2.2	20	386
1.0	10.68	5.28	16.6	218.5	8.1	3.8	20	3.11×10^3
2.0	10.92	5.35	7.4	224.2	8.8	4.05	20	1.12×10^4
5.0	11.05	5.39	2.2	227.2	9.1	4.4	20	6.81×10^4
10.0	11.11	5.41	1.0	228.9	9.1	4.5	20	2.75×10^5

Table II. Average energy (in MeV) of axions emitted from the axion sphere at times from 0.05 sec to 20 sec, for $k = 0.1$, 0.3, and 1, and axion masses from 10^{-2} eV to 10 eV.

m_a(eV)	50 ms	100 ms	500 ms	1.0 sec	5.0 sec	10.0 sec	20.0 sec
			k = 0.3				
0.01	0.0	0.0	0.0	0.0	0.0	0.0	0.0
0.03	15.6	16.3	21.2	20.8	17.0	9.2	
0.1	38.3	57.0	68.0	49.0	19.0	10.6	6.4
0.3	79.0	76.6	52.0	44.0	20.5	12.6	6.8
1.0	56.0	45.4	22.5	22.2	14.0	10.7	7.0
2.0	43.5	28.0	12.0	14.0	10.5	8.2	6.1
3.0	37.2	20.8	10.7	10.4	9.0	7.3	5.4
5.0	29.0	14.7	9.5	9.0	7.3	5.8	4.4
10.0	19.8	11.3	6.8	7.0	5.7	4.6	3.5
			k = 0.1				
0.01	0.0	0.0	0.0	0.0	0.0	0.0	0.0
0.03	15.5	16.5	19.0	18.3	13.5	8.3	
0.1	47.2	65.8	47.9	35.5	15.0	8.1	
0.3	79.0	75.8	49.3	38.8	16.0	9.5	5.5
1.0	56.0	45.5	22.0	21.2	15.0	10.5	6.6
2.0	43.5	27.9	13.8	14.5	10.3	8.0	5.7
10.0	20.0	11.3	7.2	7.0	5.2	4.2	3.2
			k = 1.0				
0.01	0.0	0.0	0.0	0.0	0.0	0.0	0.0
0.03	15.6	15.9	24.0	24.7	21.5	11.6	
0.1	39.0	53.8	84.4	67.4	25.3	14.0	
0.3	80.0	77.0	53.0	47.0	25.0	15.7	8.7
1.0	56.0	45.4	23.0	22.2	15.5	11.5	8.0
2.0	43.5	28.0	14.5	14.0	10.2	8.3	6.2